



Contents lists available at ScienceDirect

Journal of Environmental Radioactivity

journal homepage: www.elsevier.com/locate/jenvrad

World Meteorological Organization's model simulations of the radionuclide dispersion and deposition from the Fukushima Daiichi nuclear power plant accident[☆]



Roland Draxler^{a,*}, Dèlia Arnold^e, Masamichi Chino^g, Stefano Galmarini^f, Matthew Hort^b, Andrew Jones^b, Susan Leadbetter^b, Alain Malo^c, Christian Maurer^e, Glenn Rolph^a, Kazuo Saito^d, René Servranckx^c, Toshiki Shimbori^d, Efisio Solazzo^f, Gerhard Wotawa^e

^a National Oceanic and Atmospheric Administration, College Park, MD 20740, USA

^b Met Office, Exeter, United Kingdom

^c Canadian Meteorological Centre, Montréal, Canada

^d Japan Meteorological Agency, Ibaraki, Japan

^e Zentralanstalt für Meteorologie und Geodynamik, Vienna, Austria

^f European Commission, Joint Research Centre, Ispra, Italy

^g Japan Atomic Energy Agency, Ibaraki, Japan

ARTICLE INFO

Article history:

Received 24 May 2013

Received in revised form

23 September 2013

Accepted 26 September 2013

Available online 31 October 2013

Keywords:

Fukushima

Deposition

Air concentration

ATDM

Iodine

Cesium

ABSTRACT

Five different atmospheric transport and dispersion model's (ATDM) deposition and air concentration results for atmospheric releases from the Fukushima Daiichi nuclear power plant accident were evaluated over Japan using regional ¹³⁷Cs deposition measurements and ¹³⁷Cs and ¹³¹I air concentration time series at one location about 110 km from the plant. Some of the ATDMs used the same and others different meteorological data consistent with their normal operating practices. There were four global meteorological analyses data sets available and two regional high-resolution analyses. Not all of the ATDMs were able to use all of the meteorological data combinations. The ATDMs were configured identically as much as possible with respect to the release duration, release height, concentration grid size, and averaging time. However, each ATDM retained its unique treatment of the vertical velocity field and the wet and dry deposition, one of the largest uncertainties in these calculations. There were 18 ATDM-meteorology combinations available for evaluation. The deposition results showed that even when using the same meteorological analysis, each ATDM can produce quite different deposition patterns. The better calculations in terms of both deposition and air concentration were associated with the smoother ATDM deposition patterns. The best model with respect to the deposition was not always the best model with respect to air concentrations. The use of high-resolution mesoscale analyses improved ATDM performance; however, high-resolution precipitation analyses did not improve ATDM predictions. Although some ATDMs could be identified as better performers for either deposition or air concentration calculations, overall, the ensemble mean of a subset of better performing members provided more consistent results for both types of calculations.

Published by Elsevier Ltd.

[☆] This is an open access article under the CC BY license (<http://creativecommons.org/licenses/by/3.0/>).

* Corresponding author. Tel.: +1 301 683 1372; fax: +1 301 683 1370.

E-mail address: Roland.Draxler@noaa.gov (R. Draxler).

1. Introduction

The World Meteorological Organization (WMO) organized an effort to assist the United Nations Scientific Committee on the Effects of Atomic Radiation (UNSCEAR) in its assessment of the Fukushima Daiichi accident. The WMO convened a small Task Team (TT) consisting of experts from Japan, United Kingdom, Canada, Austria, and the United States to examine how the use of meteorological analyses and additional meteorological observations could improve atmospheric transport, dispersion and deposition

calculations for effluents released into the atmosphere during the Fukushima Daiichi nuclear power plant accident.

A summary of the meteorological conditions during the critical phases of the atmospheric emissions is given in the WMO TT report (WMO, 2013) and by several other researchers (Morino et al., 2011; Kinoshita et al., 2011; Stohl et al., 2012; Sugiyama et al., 2012). Briefly, from March 9th to 12th a weak low pressure trough over eastern Japan caused light rain to be observed. Then a high pressure system moved eastward along the south coast of the main island of Japan from the 12th through the 13th. From March 14th to 15th another weak low pressure trough moved eastward off the southern coast of the main island then moved toward the northeast while developing rapidly after the 15th. In particular, rain was observed in the Fukushima prefecture during the night from 1700 JST¹ March 15 to 0400 JST March 16 (Kinoshita et al., 2011), a time corresponding with significant emissions. High pressure dominated on March 18th and 19th and the winds were generally from the west. A low pressure system passed over the main island from March 20th to the 22nd causing moderate rain near Tokyo.

Several modeling studies have already been conducted, from the local scale examining the major contamination episode of March 15th (Chino et al., 2011), to a more regional scale simulation covering Japan (Morino et al., 2011; Yasunari et al., 2011; Katata et al., 2012; Le Petit et al., 2012), and to the global scale (Takemura et al., 2011; Stohl et al., 2012; Christoudias and Lelieveld, 2013). The modeling results generally support the case that the high-deposition area over the middle of the Fukushima prefecture was primarily caused by the deposition that occurred on March 15th.

For the WMO evaluation, each TT member ran their organization's atmospheric transport, dispersion and deposition model (ATDM) with the various meteorological data available. All calculations were made using a unit emission and divided into independent 3-h emission segments. Air concentration and deposition was calculated after the more time consuming transport and dispersion calculations were completed by multiplying the model results by the time-varying emission rates and decay rates for each species. As part of the evaluation, predictions from each of the ATDM calculations as well as the ensemble mean calculation were compared to the observed ¹³⁷Cs deposition pattern and the time series of ¹³⁷Cs and ¹³¹I air concentrations at a single downwind location.

2. Atmospheric transport and dispersion models

The meteorological evaluation of the Fukushima accident was sponsored by the WMO and the TT members were all from countries participating in the WMO emergency response program. The ATDMs used by the TT members included MLDPO (*Modèle Lagrangien de Dispersion de Particules d'ordre 0* – Canada), HYSPLIT (Hybrid Single-Particle Lagrangian Integrated Trajectory Model – United States), NAME (Numerical Atmospheric-dispersion Modelling Environment – United Kingdom), RATM (Regional Atmospheric Transport Model – Japan), and FLEXPART (Lagrangian Particle Dispersion Model – Austria). All the ATDMs are of a class of models called Lagrangian Particle Dispersion Models (LPDMs). The transport and dispersion of individual pollutant particles or gases are simulated in a computational framework that follows the position of the individual element by its mean motion from the wind fields and a turbulent component to represent the dispersion.

These models are all run off-line, meaning that the meteorological fields need to be available as input to the ATDM.

MLDPO is a dispersion model designed for long-range dispersion problems occurring at regional and global scales (D'Amours and Malo, 2004; D'Amours et al., 2010). Wet deposition is treated with a simple wet scavenging rate scheme and occurs when a particle is in a cloud. Below-cloud scavenging is not considered in the operational version of MLDPO. In contrast to all the other ATDMs the precipitation field is not used directly by MLDPO, but the tracer removal rate is proportional to the local cloud fraction and particle mass.

HYSPLIT is described in more detail by Draxler and Hess (1997, 1998). Similar to many of the other ATDMs, wet scavenging is parameterized through exponential removal constants where the deposition each time step depends upon the particle mass and precipitation rate. For in-cloud processes, a scavenging coefficient is defined, the ratio of the pollutant's concentration in water to its concentration in air. Below-cloud removal is defined directly as a rate constant, independent of the precipitation rate. The wet deposition of gases depends upon their solubility and for inert non-reactive gases it is a function of the Henry's Law constant, the ratio of the pollutant's equilibrium concentration in water to that in air.

NAME is used to model the atmospheric transport and dispersion of a range of gases and particles (Maryon et al., 1999; Jones et al., 2007). The removal of material from the atmosphere by wet deposition is based on the air concentration and a scavenging coefficient that depends upon the rainfall rate and two coefficients which vary for different types of precipitation (large-scale or convective and rain or snow) and for different wet deposition processes. Wet deposition due to convective and large-scale precipitation is computed separately and summed to give total wet deposition. Material located above the cloud top is not subject to wet deposition. Enhanced wet deposition is applied to material close to the ground in regions of elevated orography.

RATM is the tracer transport model designed to be driven by the mesoscale analysis data. The original version of RATM has been used for operational products at JMA including photochemical oxidants and tephra fall forecasts. The model description can be found in Shimbori et al. (2010) and Saito (2012). The treatment of radionuclides is a new application implemented for the WMO TT evaluation. The removal of material by wet deposition is also given by a below-cloud scavenging rate (Kitada, 1994) which depends upon the precipitation intensity. Wet deposition for gases is considered only as an in-cloud scavenging rate (Hertel et al., 1995) which depends upon the liquid water content, temperature, and cloud thickness. Wet deposition is applied only for particles or gases below 1500 m.

FLEXPART (Stohl et al., 1998, 2005) is applied to many different atmospheric transport modeling applications, ranging from emergency response, research, and nuclear releases (Stohl et al., 2012). As with the other ATDMs, deposition processes are expressed by a loss of mass through an exponential decay of the particle mass and where the scavenging coefficients have a different formulation and user supplied values, for below-cloud scavenging (following McMahon and Denison, 1979), in-cloud scavenging (following Hertel et al., 1995), or species type such as gases or aerosols.

3. Meteorological analysis data

There were four global meteorological analyses data sets available (Canada, United States, European Center, UK Met Office) and two regional high-resolution analyses (Japan) for use by the ATDMs.

The Canadian Meteorological Centre (CMC) is part of the Meteorological Service of Canada and is the national center for

¹ JST (Japan Standard Time) = UTC + 9 h, i.e. JST is 9 h ahead of Coordinated Universal Time (UTC).

numerical weather prediction (NWP). CMC runs operationally a complete integrated suite of NWP models under an infrastructure called the Global Environmental Multiscale (GEM) system (Côté et al., 1998a,b). The GEM system executed in a global configuration is called the Global Deterministic Prediction System (GDPS, CMC, 2009; Bélair et al., 2009; Charron et al., 2012). The GDPS includes a 4D variational data assimilation system and is run twice a day (00 and 12 UTC). Analyses are available at a 6-h frequency at 00, 06, 12, 18 UTC. The horizontal grid mesh of the GDPS is defined at 33 km (0.3° horizontal resolution)² and the vertical discretization is over 80 hybrid-pressure levels. A post-processing task of the GDPS interpolates the data from the native hybrid-pressure coordinate system to the standard eta coordinate system on 58 vertical levels. This global meteorological analyses database is used to drive MLDPO. A total of 30 eta vertical levels were selected for the ATDM calculations including 14 levels within the 2-km above ground layer (AGL; below ~800 hPa) in order to resolve properly physical processes taking place in the atmospheric boundary layer.

The National Oceanic and Atmospheric Administration's (NOAA) National Weather Service's National Centers for Environmental Prediction (NCEP) runs a series of computer analyses and forecasts operationally. One of the systems is the GDAS (Global Data Assimilation System) which is part of the Global Forecast System (Kanamitsu, 1989; Kanamitsu et al., 1991). The GDAS is run 4 times a day (00, 06, 12, and 18 UTC). Model output is for the analysis time and 3, 6, and 9-h forecasts. Post-processing of the GDAS converts the data from spectral coefficient form to half degree latitude-longitude grids and from sigma levels to mandatory pressure levels. The successive analyses and 3-h forecasts four times each day produce a continuous data archive. The NOAA ATDM used the GDAS data on the native hybrid vertical coordinate system and calculations by the Zentralanstalt für Meteorologie und Geodynamik's (ZAMG) FLEXPART also used the GDAS data, but on isobaric levels.

The European Centre for Medium-Range Weather Forecasts (ECMWF) produces a high-resolution global forecast twice daily at 00 UTC and 12 UTC. It is a spectral NWP model (Simmons et al., 1989) using a 4D variational data assimilation system (4D-Var), see Rabier et al. (2000) and Mahfouf and Rabier (2000) with 91 vertical levels. Archived model fields have been extracted from the ECMWF archive at a temporal resolution of 3 h as a sequence of short-period forecasts from successive forecast cycles of the operational global model. Meteorological fields were retrieved by the UK Met Office on a regular latitude-longitude grid at 0.125° by 0.125° resolution for use by NAME and HYSPLIT, and at 0.2° by 0.2° resolution by ZAMG for FLEXPART over a region centered on Japan.

The operational global configuration of the Met Office Unified Model, MetUM (Davies et al., 2005) was only used for calculations with NAME. The global version of the Unified Model uses an incremental 4D-Var. Forecasts are produced on a 6-h cycle to give four forecast runs per day. Model fields are output for NAME at a temporal resolution of 3 h, and archive data therefore consist of alternating model analyses and 3-h forecasts. Meteorological fields from the global model have an approximate horizontal resolution of 25 km in the mid-latitudes, with 70 vertical levels extending to an altitude of 80 km (but only the lowest 59 model levels up to approximately 30 km are used for NAME applications). Meteorological data is interpolated in both space and time within NAME.

The Japan Meteorological Agency (JMA) provided their meso-scale analyses fields for the period 11–31 March 2011, at three-

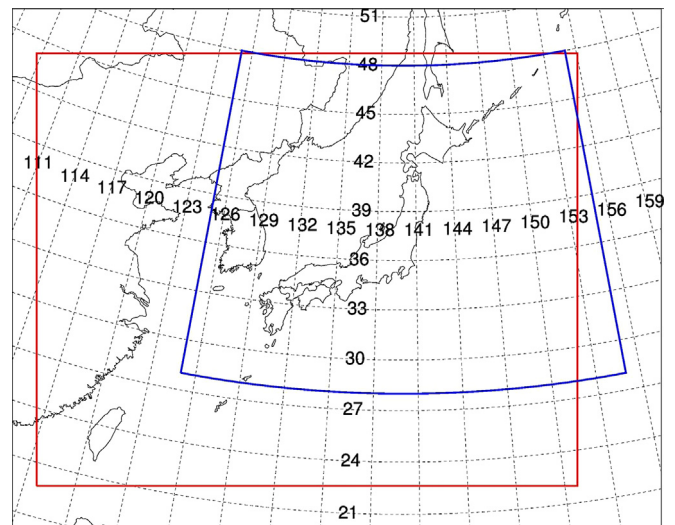


Fig. 1. The larger red box shows the domain of the JMA mesoscale analysis on its Lambert Conformal projection and the inner blue box shows the latitude–longitude air concentration and deposition grid. Calculations occur within the meteorological data grid. (For interpretation of the references to color in this figure legend, the reader is referred to the web version of this article.)

hourly intervals and at a 5-km horizontal resolution. The meso-scale analyses (MESO) are produced by the operational non-hydrostatic 4D-Var system of JMA and it assimilates a variety of local meteorological observations, including GPS-derived total precipitable water vapor and radar/rain gauge-analyzed precipitation (RAP; see Honda et al., 2005; Saito et al., 2007; Honda and Sawada, 2008 for more detailed discussions). The MESO domain covered a region of about 3000 by 3000 km on a Lambert Conformal projection (see Fig. 1) with 50 levels up to about 21 km above ground.

It was recognized that perhaps the most critical element in the deposition calculations was getting the precipitation correct, and the incorporation of the JMA radar/rain gauge-analyzed precipitation fields (RAP, available every 30 min at 1-km resolution) was essential to the resulting deposition computations. JMA also provided the RAP dataset (Nagata, 2011), independently of the MESO analysis, at 30 min intervals, with a horizontal resolution of 45 s in longitude and 30 s in latitude covering a region from 118 to 150° east longitude and from 20 to 48° north latitude. A more detailed discussion of the JMA precipitation is given by Saito et al. (2014). Several of the ATDM calculations used global meteorological analysis in combination with the high-resolution radar–rain gauge precipitation, essentially replacing the model precipitation field with the RAP precipitation rate, for the wet deposition calculation.

The analysis data characteristics are briefly summarized in Table 1. Each member of the TT would run their ATDM with the meteorological data they normally use for operational dispersion predictions and also, if technically possible, one or more of the other analyses. Not all of the ATDMs were able to use all of the meteorological data combinations depending upon the level of ATDM code modification required to use different analyses. The 18 completed ATDM–meteorology combinations are listed Table 2.

4. ATDM simulation configuration

All the ATDMs were configured identically as much as possible in terms of the dispersion and deposition configuration such as release duration, height, concentration grid size and time resolution. Each ATDM retained its unique treatment of wet and dry

² The GDPS horizontal grid mesh has been changed to 25 km in February 13th 2013 (for additional details: http://collaboration.cmc.ec.gc.ca/cmc/cmof/product_guide/docs/lib/op_systems/doc_opchanges/technote_gdps300_20130213_e.pdf).

Table 1
Summary of the meteorological analyses fields available for the ATDM calculations.

Meteorological Center's product	Acronym	Space	Time	Vertical
CMC's Global Environmental Multiscale system	GEM	0.30°	6 h	Sigma
NOAA's Global Data Assimilation System	GDAS	0.50°	3 h	Hybrid sigma
The European Centre for Medium-Range Weather Forecasts	ECMWF	0.125° and 0.2°	3 h	Hybrid sigma
UKMET's operational global Unified Model	MetUM	0.23° by 0.35°	3 h	Height levels
JMA's mesoscale analyses fields	MESO	5 km	3 h	Hybrid height levels
JMA's radar–rain gauge-analyzed precipitation	RAP	1 km	30 min	Surface

Table 2
ATDM-meteorology simulations completed (C) by each participating ATDM model (rows) with different meteorological data (columns) and also the ATDM simulations enhanced with the RAP data (R).

Data/model	CMC	NOAA	ECMWF	MetUM	JMA
CMC-MLDP0	C				C
JMA-RATM					C, R
NOAA-HYSPLIT		C, R	C, R		C, R
UKMET-NAME			C	C	C, R
ZAMG-FLEXPART		C, R	C, R		

deposition, one of the largest uncertainties in these calculations and thereby providing for a range of possible solutions. In general, these ATDMs use comparable transport and dispersion schemes that are primarily dependent upon the input meteorological data. However, one other significant difference between the ATDMs was the treatment of the vertical velocity field in the MESO analysis. In the CMC model the field was not used but diagnosed from the divergence, in the JMA model the field was first spatially averaged and the lowest velocity set to zero, while the UKMET and NOAA models used the field directly after conversion to a terrain following coordinate.

The ATDM air concentration and deposition output fields were configured to use a regular latitude-longitude grid (601 by 401 grid cells) with the output averaged at 3-hourly intervals at 0.05° (5 km) horizontal resolution and 100 m vertical resolution. The domain was over the northeast corner of the JMA mesoscale analysis grid (see Fig. 1). In all ATDM calculations, particles that exited the concentration grid may still be on one of the meteorological data grids and computations would continue until the particle was terminated due to exceeding its maximum age (72 h) or exiting the meteorological grid. The simulations are conducted for the period 11 through 31 March 2011.

To allow maximum flexibility regarding the release rates of key nuclides, the computations were based on the concept of source-receptor matrices, in this connection also called transfer coefficient matrices (TCM – Draxler and Rolph, 2012). Each 3-h release period was treated as an independent computation. The period of 11–31 March required 168 simulations. The 72 h maximum particle duration was selected to speed up the regional dispersion computations for ATDMs using global meteorological data.

Computations were done using a unit release rate (1 Bq/h) assuming the emissions were uniformly distributed from the ground to 100 m AGL. The initial uniform vertical distribution was a compromise solution for the unknown variations in release height. Three generic species were tracked as surrogates for the radionuclides: a gas with no wet or dry scavenging (non-depositing gas),³ a gas with a relatively large dry deposition velocity and wet removal to represent gaseous ¹³¹I (depositing gas), and a particle with a small deposition velocity (light particle) to represent the remaining

radionuclides, such as ¹³⁷Cs for example. In this way the calculations could be post-processed for the air concentration and deposition for most radionuclides emitted from a reactor accident without any prior knowledge of the detailed emissions scenario. In the post-processing step, the results from each ATDM simulation would be multiplied by the actual emission rate and decay constant for the radionuclide desired. The individual simulation results are then added together for each output time period.

The TCM approach easily permits the testing of multiple emission scenarios. For the results shown here, the emissions originally derived by Chino et al. (2011) and later modified by Terada et al. (2012) are used. The emission rates were aggregated into 168 values representing the hourly emission rate for each simulation valid over one 3 h emission period (Fig. 2). To assist the TT evaluation efforts, a web interface (http://ready.arl.noaa.gov/READY_fdnpwmo.php) was designed to permit the selection of the ATDM, emission rate, radionuclide, and measurement data. The web interface output provides graphical results in a common format for all models, model performance statistics compared with measurement data, and various output options from the native binary, text based, or NetCDF.

5. Measurement data for model evaluation

The TT concluded that the best overall metric would be to evaluate the ATDM's performance with each meteorological data combination by comparing the model predicted patterns of ¹³⁷Cs deposition to the available deposition measurements. The accumulated ¹³⁷Cs deposition field has the advantage of providing measurements over a wide region. One disadvantage is that the bulk of the deposition occurred during only a few time periods associated with precipitation. In addition, there is considerable interest in how well the ATDM-meteorology combinations can represent the air concentration data. However, in terms of radionuclide specific measurements, air concentration data were available at only a few locations. The more abundant gamma dose measurements were not used due to their dependence upon detailed knowledge of the emissions of multiple species contributing to the dose as well as the complicating effects of previously accumulated deposition on the current dose measurement.

To perform a quantitative analysis of the ATDM-meteorology combinations requires a digital version of the now frequently reproduced ¹³⁷Cs deposition graphic first reported by the Japanese Ministry of Education, Culture, Sports and Science and Technology (MEXT) and subsequently published (Kinoshita et al., 2011). However, only some of the measurements contributing to this graphic are available in digital form and they have been merged into an equivalent product that is used for the ATDM-meteorology evaluations. The version used here includes measurements taken by the U.S. Department of Energy's (USDOE, 2011) fixed-wing aircraft from 2 April 2011 to 9 May 2011 and ground-based measurements by MEXT (MEXT, 2011). It is assumed that the data collected early in the period (2 April) could be used as proxy for the total deposition on 31 March (end of the modeling period). The collected aircraft

³ Non-depositing gases are used to mimic noble gases, such as ¹³³Xe.

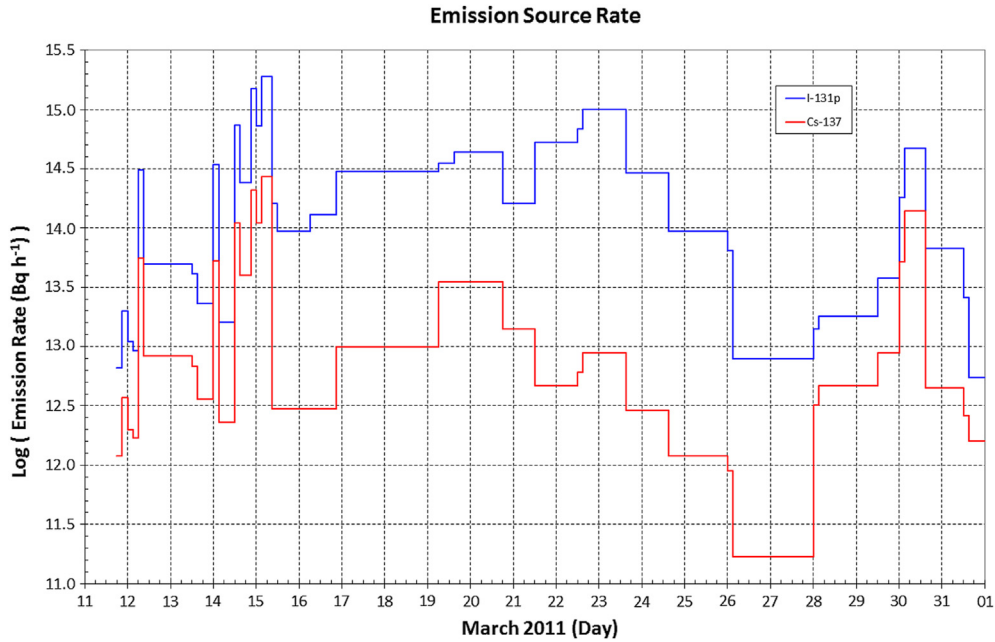


Fig. 2. The time-varying emissions in Becquerel per hour at 3 h intervals for ¹³⁷Cs (red line) and particulate ¹³¹I (blue line) used for the ATDM-meteorology evaluations. (For interpretation of the references to color in this figure legend, the reader is referred to the web version of this article.)

and ground-based data points were averaged onto an identical grid (0.05° resolution) to that used in the ATDM calculations. The aircraft based sampling covered 374 grid points and blending in the additional ground-based data resulted in a total 543 deposition grid points. The blended ¹³⁷Cs deposition measurements are shown in Fig. 3. Although the spatial coverage is more limited than some of the other published data, the blended measurement data captures the primary deposition maximum in the Fukushima prefecture. Also note how the deposition is limited by the elevated terrain to the west of Fukushima.

After the accident at the Fukushima Daiichi Nuclear Power Plant, radiation was monitored at the Nuclear Fuel Cycle Engineering

Laboratories, Japan Atomic Energy Agency (JAEA). Furuta et al. (2011) and Ohkura et al. (2012) provide a summary of the monitoring results of dose rates, air concentrations, and deposition. The TT used the time series of ¹³⁷Cs and ¹³¹I air concentrations measured by JAEA at Tokai-mura (36.4356N, 140.6025E, about 110 km SSW of Fukushima Daiichi NPP, see location Tm on Fig. 3) for the ATDM-meteorology evaluations for the period of 11–31 March. Compared with the more extensive deposition measurements, only 41 samples of 9–12 h duration each were available for analysis.

We also examined the data at the Comprehensive Test Ban Treaty Organization (CTBTO) Takasaki site (<http://www.ctbto.org/verification-regime/the-11-march-japan-disaster/>) and in general

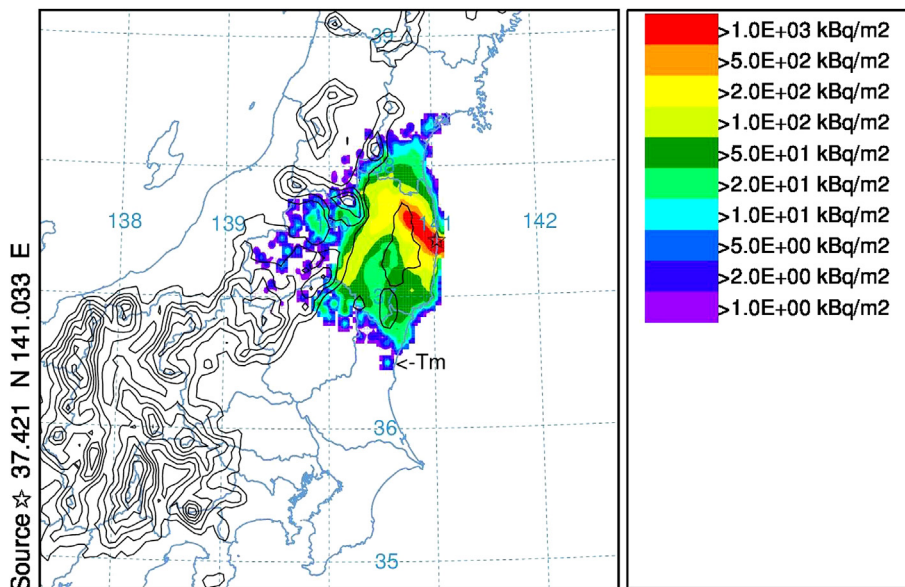


Fig. 3. Measured ¹³⁷Cs deposition based upon aerial and ground-based sampling. The solid dark lines show the terrain contours at 250 m intervals (to 2000 m) as derived from the JMA mesoscale analysis. The arrow with the Tm label points to the Tokai-mura air concentration sampling location.

Table 3

ATDM performance for the total ^{137}Cs deposition for each ATDM combination and the 10-model select ensemble (*) and the ensemble using all 18 members.

Center	Variation	CC	NMSE	FB	FMS	KSP	Rank
CMC*	GEM	0.75	6.16	-0.32	100	19	3.22
CMC*	MESO	0.76	8.88	-0.44	100	6	3.29
JMA*	MESO	0.71	4.81	-0.04	100	10	3.38
JMA*	MESO-RAP	0.84	3.79	0.56	100	13	3.29
NOAA*	ECMWF	0.83	4.20	-0.30	100	10	3.44
NOAA	ECMWF-RAP	0.55	14.09	-0.74	100	33	2.60
NOAA*	GDAS	0.87	2.59	-0.08	100	6	3.65
NOAA	GDAS-RAP	0.67	9.72	-0.57	100	23	2.94
NOAA	MESO	0.56	5.91	0.38	100	15	2.97
NOAA	MESO-RAP	0.48	7.35	0.43	100	16	2.86
UKMET	UM	0.46	8.14	0.24	100	30	2.80
UKMET*	ECMWF	0.80	2.87	0.11	100	25	3.34
UKMET	MESO	0.76	3.86	0.04	100	11	3.45
UKMET*	MESO-RAP	0.66	4.86	0.03	100	9	3.33
ZAMG*	GDAS	0.67	12.69	-0.59	100	10	3.05
ZAMG	GDAS-RAP	0.66	18.32	-0.84	100	20	2.82
ZAMG	ECMWF	0.78	3.84	-0.08	100	15	3.42
ZAMG*	ECMWF-RAP	0.83	2.55	0.13	100	6	3.56
Ensemble	All	0.85	3.27	-0.04	100	13	3.57
Ensemble*	Select	0.89	2.65	-0.04	100	15	3.62

the ATDM results were similar to those at Tokai-mura. However, because the ATDM plumes did not intersect the site as frequently, it was not as good as Tokai-mura for model evaluation purposes. Note that the ATDM results can be extracted for any location from the previously cited URL (http://ready.arl.noaa.gov/READY_fdnppwmo.php).

6. Performance measures

Procedures for evaluating ATDM calculations have a long history (Fox, 1984; Hanna, 1989, 1993; Chang and Hanna, 2004). The problem eludes simple solutions because the variability in atmospheric motions cannot be deterministically represented in any model resulting in the inevitable mismatches between predicted and measured concentrations paired in space and time. The ATDM-meteorology evaluation protocol used here follows the procedures used by Mosca et al. (1998) and Stohl et al. (1998). Both Mosca et al. (1998) and Stohl et al. (1998) recognized the problem in dealing with the uncertainties of “near background” measurement data and avoiding statistical parameters that may be too sensitive to small variations in the measurement values such as ratios between measured and calculated concentration. For a quick evaluation comparison, it is desirable to have a single parameter, which could be used to determine an overall degree of model performance. Stohl et al. (1998) found that the ratio based statistics are the most sensitive to measurement errors while the correlation coefficient is one of the most robust. Chang and Hanna (2004) are more critical of the correlation coefficient due to its sensitivity to high concentrations. Chang and Hanna (2004) also summarized attempts by several different researchers to define a single model evaluation parameter, such as ranking models by each statistic and then ordering by the total rank. In our analysis only five statistical parameters were selected to represent different evaluation metrics: the correlation coefficient (CC), the fractional bias (FB), the figure-of-merit in space (FMS), the Kolmogorov–Smirnov parameter (KSP), and the normalized mean square error (NMSE). Also a new ranking method (Draxler, 2006) was defined using the first four statistics by giving equal weight to the normalized (0–1) sum of the CC, FB, FMS, and KSP, such that the total model rank would range from 0 to 4 (from worst to best).

Table 4

ATDM performance for the ^{137}Cs air concentrations at Tokai-mura by model and for both the 10- and 18-member ensembles. The bold highlight shows the ATDM-meteorology combination with the best performance for each metric.

Center	Variation	CC	NMSE	FB	FMS	KSP	Rank
CMC*	GEM	0.10	70.86	-1.37	77.5	54	1.56
CMC*	MESO	0.26	15.24	-0.09	82.5	34	2.51
JMA*	MESO	0.45	16.43	-0.40	77.5	44	2.34
JMA*	MESO-RAP	0.11	156.29	-1.68	65.0	69	1.13
NOAA*	ECMWF	0.32	62.96	-1.34	67.5	61	1.50
NOAA	ECMWF-RAP	0.32	64.29	-1.35	67.5	61	1.49
NOAA*	GDAS	0.32	71.23	-1.37	62.5	71	1.34
NOAA	GDAS-RAP	0.32	72.67	-1.38	62.5	68	1.36
NOAA	MESO	0.18	128.54	-1.63	65.0	68	1.19
NOAA	MESO-RAP	0.18	127.89	-1.63	62.5	69	1.16
UKMET	UM	0.10	78.35	-1.42	72.5	54	1.49
UKMET*	ECMWF	0.17	35.91	-0.93	77.5	54	1.80
UKMET	MESO	0.29	21.33	-0.50	82.5	53	2.13
UKMET*	MESO-RAP	0.29	21.95	-0.53	82.5	53	2.12
ZAMG*	GDAS	0.23	22.88	-0.37	60.0	58	1.89
ZAMG	GDAS-RAP	0.27	23.83	-0.43	60.0	56	1.90
ZAMG	ECMWF	0.21	27.93	-0.54	60.0	61	1.76
ZAMG*	ECMWF-RAP	0.18	30.81	-0.56	60.0	71	1.64
Ensemble	All	0.27	31.19	-0.88	82.5	36	2.10
Ensemble*	Select	0.30	26.77	-0.77	82.5	34	2.19

7. Results

There were 18 ATDM-meteorology combinations available for evaluation plus two more representing the ensemble mean for all 18 members and the ensemble mean for a subset of 10 select members. The ^{137}Cs deposition results are given in Table 3 by model and statistical metric. The members of the 10-member subset were selected so that each of the five ATDMs would be represented by two different meteorological analyses. The select subset members are indicated by an asterisk in Table 3. The MESO, ECMWF, GDAS, and GEM analyses are represented by four, three, two, and one member(s), respectively. Out of these 10, three meteorological analyses used the RAP for the wet deposition calculations. If one ATDM had multiple options for different meteorological combinations, the option with the highest Rank score was favored to be included in the select ensemble.

The bold highlight in Table 3 shows the ATDM-meteorology combination with the best performance for each metric. In terms of the Rank, the best performance is the NOAA ATDM with GDAS

Table 5

ATDM performance for the particulate ^{131}I air concentrations at Tokai-mura by model and for both the 10- and 18-member ensembles. The bold highlight shows the ATDM-meteorology combination with the best performance for each metric.

Center	Variation	CC	NMSE	FB	FMS	KSP	Rank
CMC*	GEM	0.11	52.64	-1.26	77.5	46	1.70
CMC*	MESO	0.34	11.18	0.12	82.5	24	2.64
JMA*	MESO	0.20	16.08	0.23	77.5	35	2.35
JMA*	MESO-RAP	0.04	49.28	-1.14	65.0	61	1.47
NOAA*	ECMWF	0.33	44.94	-1.22	67.5	54	1.64
NOAA	ECMWF-RAP	0.33	44.90	-1.22	67.5	49	1.69
NOAA*	GDAS	0.34	54.89	-1.28	62.5	66	1.44
NOAA	GDAS-RAP	0.35	55.78	-1.29	62.5	61	1.49
NOAA	MESO	0.07	50.08	-1.20	65.0	66	1.39
NOAA	MESO-RAP	0.07	49.91	-1.20	62.5	64	1.39
UKMET	UM	0.09	55.12	-1.28	72.5	54	1.55
UKMET*	ECMWF	0.21	26.76	-0.79	77.5	52	1.91
UKMET	MESO	0.30	16.03	-0.29	82.5	41	2.36
UKMET*	MESO-RAP	0.30	16.56	-0.32	82.5	44	2.31
ZAMG*	GDAS	0.24	19.46	-0.18	60.0	56	2.01
ZAMG	GDAS-RAP	0.28	20.02	-0.24	60.0	56	2.00
ZAMG	ECMWF	0.22	23.37	-0.36	60.0	54	1.93
ZAMG*	ECMWF-RAP	0.18	26.59	-0.38	60.0	64	1.80
Ensemble	All	0.26	20.64	-0.62	82.5	27	2.31
Ensemble*	Select	0.28	17.70	-0.50	82.5	27	2.39

data. With respect to FB the best combination is the UKMET-MESO-RAP calculation. The ZAMG-ECMWF-RAP simulation results in the smallest NMSE. The best CC is from the 10-member select ensemble mean. Considering the range in the Rank scores (2.60–3.65) the difference in Rank between the best member (3.65) and the ensemble-select (3.62) does not seem particularly large. In fact for most of the metrics, the ensemble-select provides comparable results to the best performing member. It is also worth noting that the 10-member ensemble provides slightly better results than the ensemble mean of all the members.

Another interesting result is that when comparing individual ATDM calculations using global data (CMC-GEM and UKMET-ECMWF) versus the same models using MESO data, all models (except NOAA-GDAS) improved (in Rank) when the MESO data are used. Also when using the RAP data for wet removal, all model results (JMA, NOAA, UKMET, ZAMG-GDAS), except ZAMG-ECMWF-RAP, were inferior to the calculations using the meteorological model derived precipitation fields. A more detailed analysis of the precipitation and related wet removal by Arnold et al. (2014) noted that although the higher resolution analyzed precipitation fields

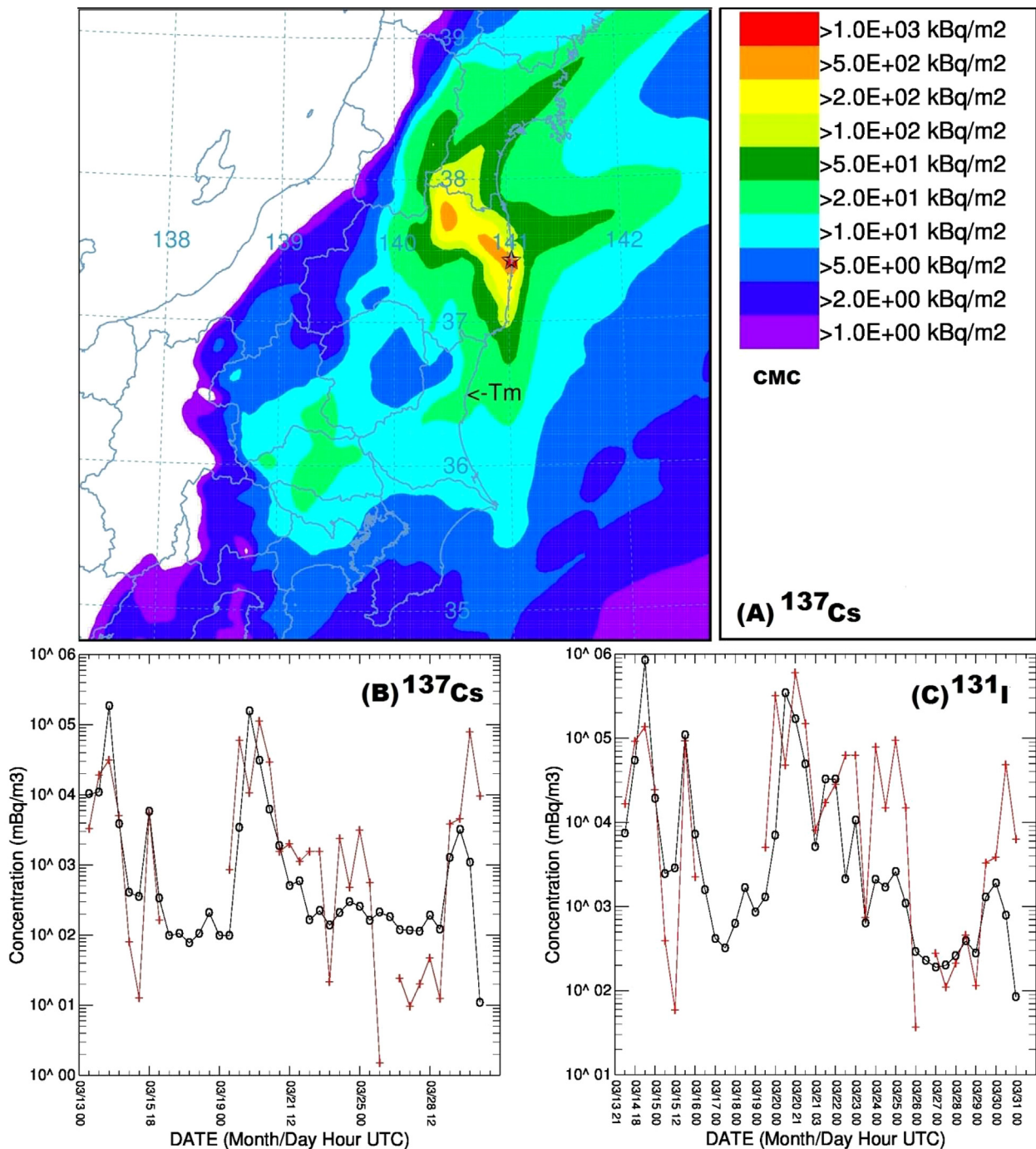


Fig. 4. Results from the CMC model using JMA mesoscale analysis data (MESO) for ^{137}Cs deposition (A), ^{137}Cs air concentrations at Tokai-mura, and particulate ^{131}I air concentrations at Tokai-mura. The arrow with the Tm label points to the air concentration sampling location. Measured values are the black lines with open circles and the model predictions are the red dashed lines with the plus symbol. (For interpretation of the references to color in this figure legend, the reader is referred to the web version of this article.)

are more accurate than model predictions of precipitation, there will be a discontinuities in both space and time between the radionuclide plumes driven by coarser resolution meteorology and the analyzed precipitation. The ZAMG modeling approach ameliorated this issue somewhat by aggregating the high-resolution precipitation into coarser spatial and temporal resolution bins.

The performance summary for ^{137}Cs air concentrations is shown in Table 4. Note that in this case the best performance over all of the metrics (except CC) comes from the CMC-MESO combination. The 10-member ensemble is 3rd in terms of Rank after the JMA-MESO calculation. Not surprisingly, the performance for air concentration is quite different from the deposition results in that one ATDM

combination dominates all the evaluation metrics. Perhaps the fact that the CMC-MESO calculation did not use the precipitation fields for the deposition calculation had a positive influence on the results compared with the other models. In terms of the other findings with respect to deposition, the air concentration results are similar, in that calculations using MESO data provide better results than using global analyses, and that the use of RAP precipitation slightly degraded the ATDM performance. The latter result is consistent with the better performance of the CMC-MESO model combination that does not directly use the precipitation fields.

The performance summary for ^{131}I particulate air concentrations is shown in Table 5. Computationally the particulate iodine is

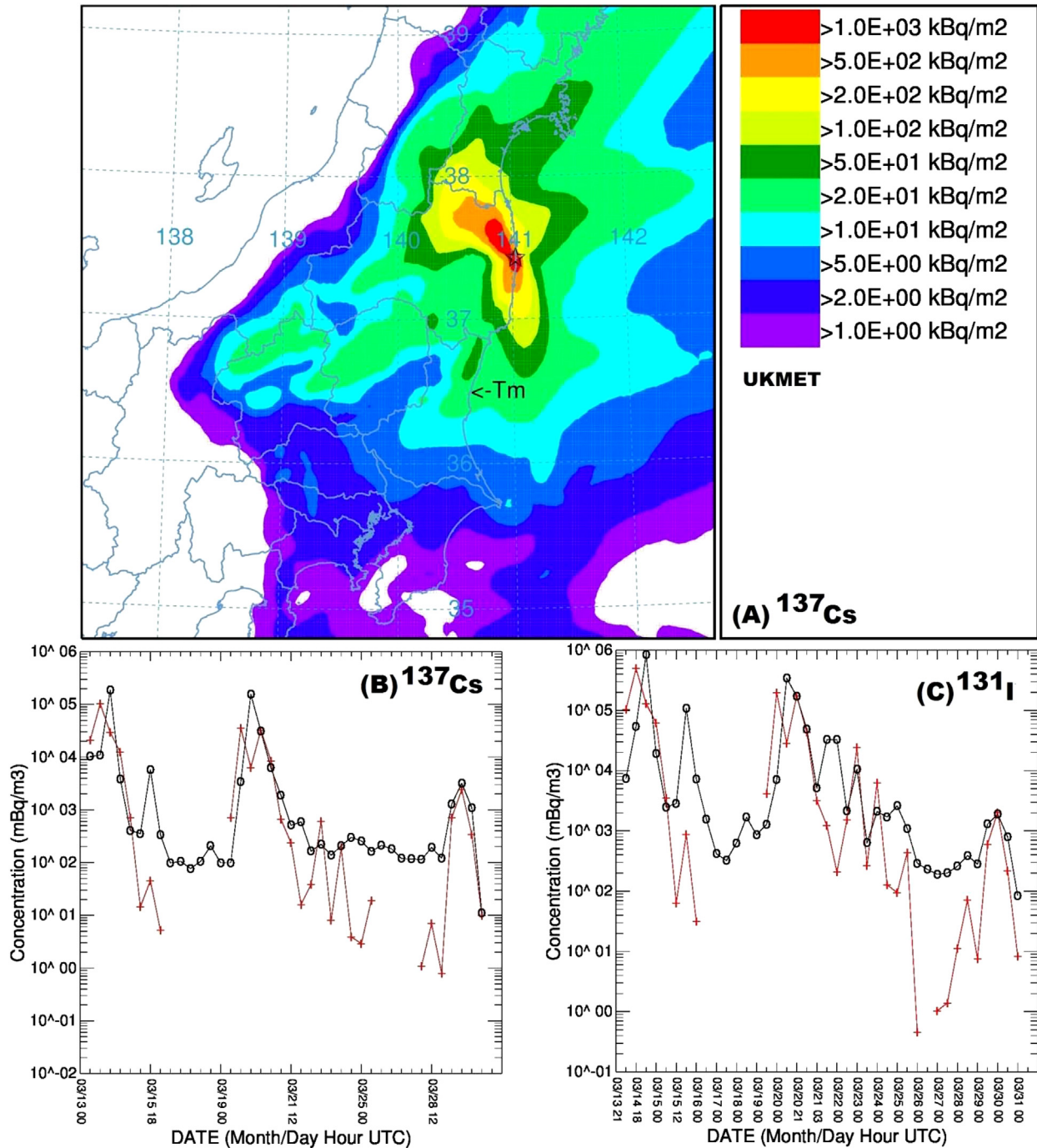


Fig. 5. Similar to Fig. 4, except showing the results from the UK Met Office model using JMA-MESO data.

treated the same way as the cesium, except for a different emissions profile and half-life. Although there are uncertainties in the gaseous to particulate release ratios of ^{131}I and potential transformations during transport, the results shown in Table 5 are very similar to the ^{137}Cs results shown in Table 4, again with the CMC-MESO calculation dominating most of the performance metrics, and the 10-member ensemble ranking second. These results are perhaps not unexpected, considering that the ^{131}I emissions were determined in part by ratios with measured ^{137}Cs (Terada et al., 2012) and differences in removal during transport may not be evident for these short-duration regional simulations.

There is an expectation that ATDM results will be different when using different meteorological analyses. However, due to differences in the way meteorological fields are processed and the way atmospheric processes are parameterized within the ATDMs, such as wet deposition, results may also differ between ATDMs when using the same meteorological data. To illustrate these differences, the deposition and air concentration time series for ^{137}Cs and particulate ^{131}I from four different models, all using the JMA-MESO analyses, are shown in Figs. 4 through 7 (CMC, UKMET, JMA, NOAA). The results show a transition from a smooth to a more granular deposition pattern between the CMC and NOAA calculations

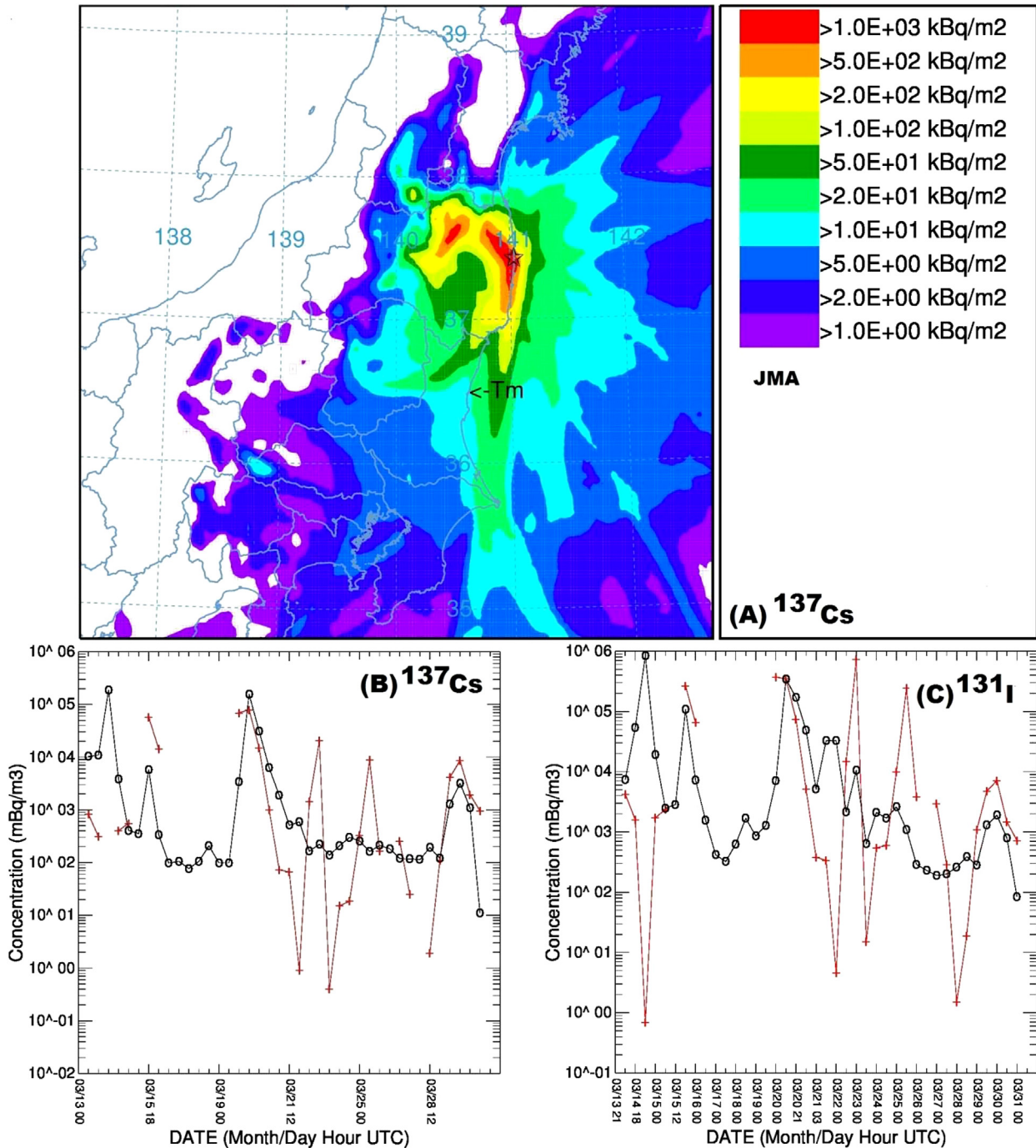


Fig. 6. Similar to Fig. 4, except showing the results from the JMA model using JMA-MESO data.

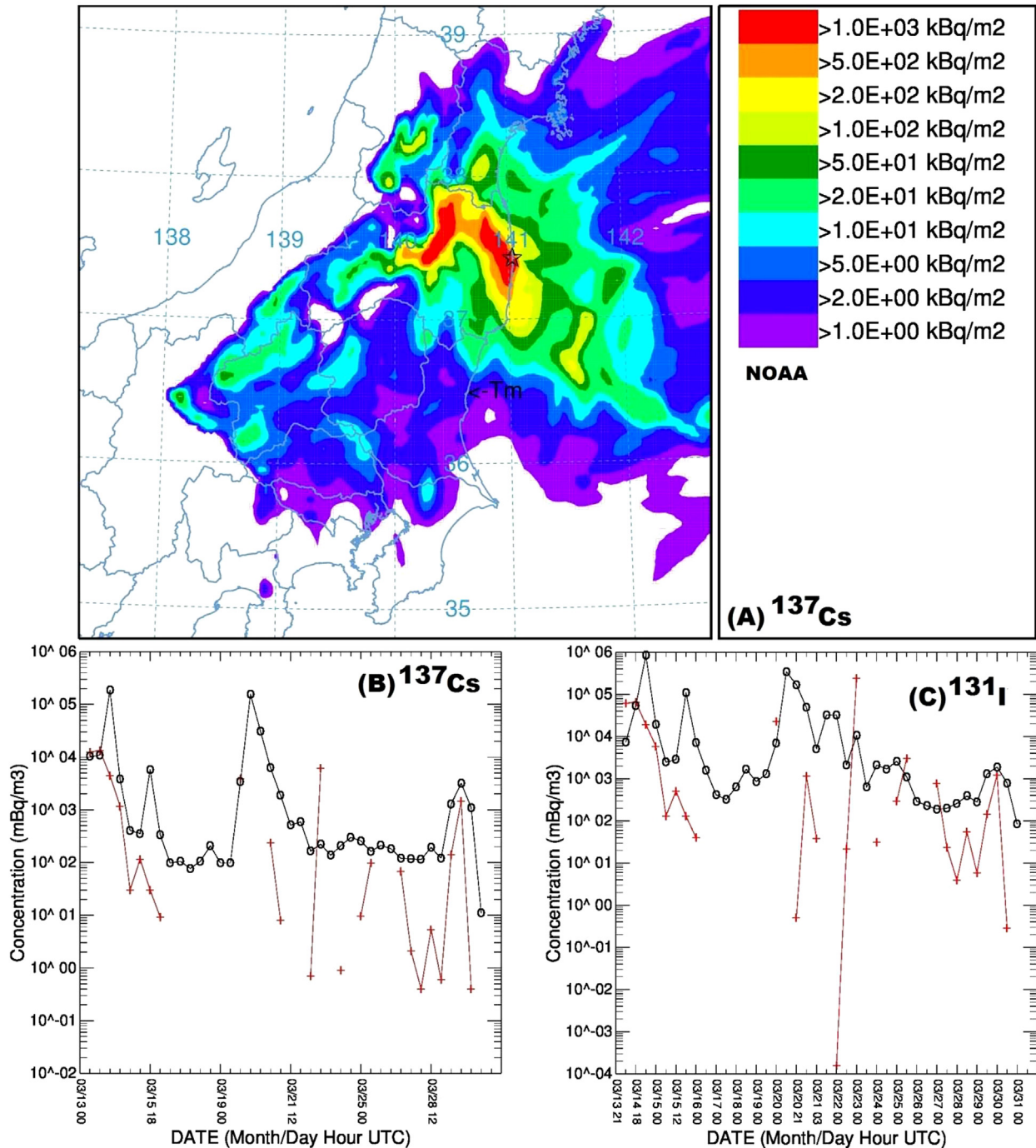


Fig. 7. Similar to Fig. 4, except showing the results from the NOAA model using JMA-MESO data.

(Figs. 4A–7A). It is interesting that although using the same meteorological analysis, each model can produce quite different patterns, perhaps understandably at the further distances from the source, but this is true even in the close-in high-deposition region. The near-source granularity is not seen in the observed deposition pattern (Fig. 3) and suggests there are benefits to smoothing some of the ATDM calculation processes and perhaps provides an additional explanation of the degradation in ATDM performance when using the RAP data.

The effect of granularity in the prediction is also evident in the air concentration time series where the smoother of the four calculations (CMC – Fig. 4B, C and UKMET – Fig. 5B, C) show a reduced

range in the magnitude of the over- and under-predictions compared with the more granular calculations (JMA – Fig. 6B, C and NOAA – Fig. 7B, C).

8. Discussion and summary

The comparison of five different ATDMs using six different meteorological analyses with measured deposition and air concentration data provided some guidance as to how multiple models (ATDM and meteorology) can provide more information than the results from any one model. There was no one ATDM-meteorology combination that provided the best results for both deposition and

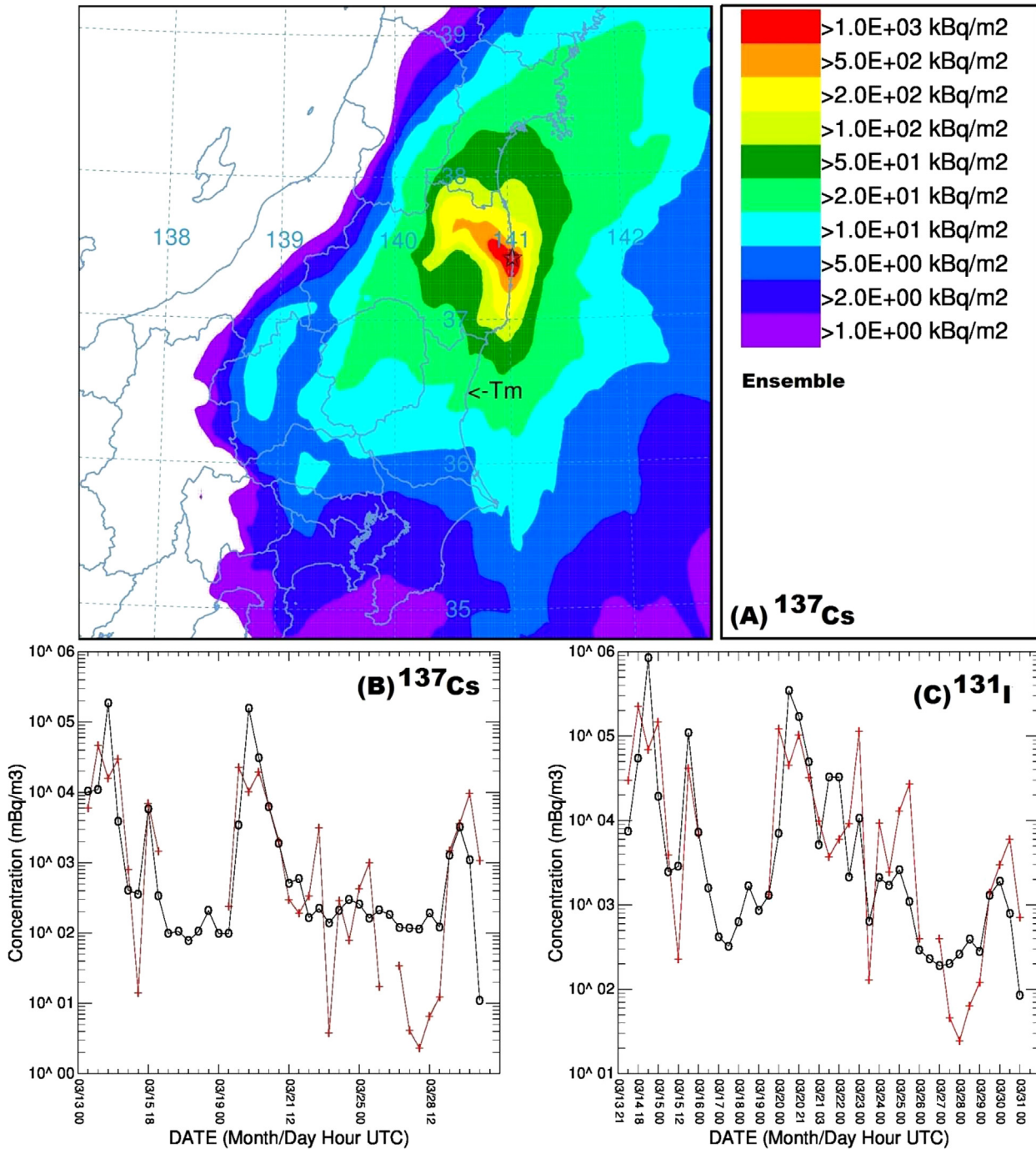


Fig. 8. Similar to Fig. 4, except the results are from the 10-model ensemble mean consisting of different ATDMs and meteorology.

air concentration predictions. In terms of deposition, several models showed good performance, depending upon the statistical metric, while for air concentration the CMC-MESO calculation performed well over several different metrics. However, the 10-member ensemble tended to be one of the top combinations for both deposition and air concentration. Comparing the CMC-MESO calculation (Fig. 4) with the 10-member ensemble (Fig. 8), the deposition patterns and concentration time series are very similar. The strength of this approach is that instead of relying upon an individual ATDM-meteorology combination, when multiple model results are available, it is possible to create an ensemble mean. In this situation, because measurement data are available, it was

possible to select a subset of models that provided a better prediction than the ensemble mean of all the models. Although there may be justification for the selection of one model, because measurement data are available in this case, there is no guarantee that the performance of the selected model will still be the best when other time periods or locations are selected that are different from the measurements used in the evaluation. Other researchers (Riccio et al., 2012) have developed more quantitative approaches to selecting ensemble members which has been applied to the Fukushima accident (Galmarini and Solazzo, 2014).

One issue not addressed directly was the sensitivity of the evaluation to the source term assumptions. The true source term

may never be known precisely. A recent study by Kobayashi et al. (2013) using marine based deposition measurements proposed substantial increases (double) in the atmospheric emissions over previously published values (Terada et al., 2012). The TCM-based calculation approach used here has a lot of merits due to its flexibility to changing the source term without rerunning the ATDMs. In the emission rates used for the evaluation (Fig. 2), one of the larger releases of ^{137}Cs ($2.1 \times 10^{14} \text{ Bq h}^{-1}$) occurred during the 3-h period starting 2100 UTC on 14 March. Increasing the emission rate for just this one time period by about a factor of four ($8.1 \times 10^{14} \text{ Bq h}^{-1}$), so that it might be more representative of a short-duration explosive event, changes the deposition performance of the 10-member ensemble mean model from a Rank of 3.62 to 3.27. This dramatic change, resulting primarily from increased bias (FB -0.04 to 0.21), can provide some interpretive guidance to the importance of the variations in Rank shown in Table 3. Considering that different meteorological data may have different wind directions during this critical time, or that different ATDMs handle the wet deposition differently, supports the argument that an ensemble mean result is preferable to any one model.

Overall, when comparing multiple ATDMs and different meteorological analyses, it was found that the use of high-resolution mesoscale analyses improved ATDM performance; however, high-resolution precipitation analyses did not improve ATDM predictions. This suggests that model performance is not just dependent upon having the best meteorology to drive the calculations, but also depends upon the pre-processing and other transformations that are required for an ATDM to use meteorological data. Although a single ATDM could be identified for either deposition or air concentration calculations, overall, the ensemble mean provided more consistent results for both types of calculations. When measurement data are available, it is possible to select a subset of models that will provide for better performance than the mean of all the models.

Acknowledgments

We thank Florian Gering from the Bundesamt für Strahlenschutz (BfS) for providing us the digitized MEXT ^{137}Cs deposition measurements; Petra Seibert from the University of Vienna for providing modifications of the FLEXPART wet deposition scheme; Teruyuki Kato of the Meteorological Research Institute of Japan and Tabito Hara and Eiji Toyoda of the Japan Meteorological Agency for providing JMA-MESO and -RAP analyses and their file conversion programs; the European Centre for Medium-Range Weather Forecasts (ECMWF) at Shinfield Park, Reading, RG2 9AX, United Kingdom for making their meteorological data analysis available, and Peter Chen and Alice Soares of the WMO Secretariat for taking the initiative to organize the effort to assist the UNSCEAR assessment and organizing the Task Team activities.

References

- Arnold, D., Maurer, C., Wotawa, G., Draxler, R., Saito, K., Seibert, P., 2014. Influence of the meteorological input on the local and global atmospheric transport of radionuclides after the Fukushima Daiichi nuclear accident. *J. Environ. Radioact.* 139, 212–225.
- Bélair, S., Roch, M., Leduc, A.-M., Vaillancourt, P.A., Laroche, S., Mailhot, J., 2009. Medium-range quantitative precipitation forecasts from Canada's new 33-km deterministic global operational system. *Wea. Forecasting* 24, 690–708. [dx.doi.org/10.1175/2008WAF2222175.1](https://doi.org/10.1175/2008WAF2222175.1).
- Chang, J.C., Hanna, S.R., 2004. Air quality model performance evaluation. *Meteorol. Atmos. Phys.* 87, 167–196. [dx.doi.org/10.1007/s00703-003-0070-7](https://doi.org/10.1007/s00703-003-0070-7).
- Charron, M., Polavarapu, S., Buehner, M., Vaillancourt, P.A., Charette, C., Roch, M., Morneau, J., Garand, L., Aparicio, J.M., MacPherson, S., Pellerin, S., St-James, J., Heilliette, S., 2012. The stratospheric extension of the Canadian global deterministic medium-range weather forecasting system and its impact on tropospheric forecasts. *Mon. Wea. Rev.* 140, 1924–1944. [dx.doi.org/10.1175/MWR-D-11-00097.1](https://doi.org/10.1175/MWR-D-11-00097.1).
- Chino, M., Nakayama, H., Nagai, H., Terada, H., Katata, G., Yamazawa, H., 2011. Preliminary estimation of release amounts of ^{131}I and ^{137}Cs accidentally discharged from the Fukushima Daiichi nuclear power plant into the atmosphere. *J. Nucl. Sci. Technol.* 48 (7), 1129–1134. [dx.doi.org/10.1080/1881248.2011.9711799](https://doi.org/10.1080/1881248.2011.9711799).
- Christoudias, T., Lelieveld, J., 2013. Modelling the global atmospheric transport and deposition of radionuclides from the Fukushima Dai-ichi nuclear accident. *Atmos. Chem. Phys.* 13, 1425–1438. [dx.doi.org/10.5194/acp-13-1425-2013](https://doi.org/10.5194/acp-13-1425-2013).
- CMC, 2009. A New Stratosphere–Troposphere Assimilation and Medium Range Forecast System for Operational Numerical Weather Prediction. Environment Canada's technical notes on operational implementations http://collaboration.cmc.ec.gc.ca/cmc/cmof/product_guide/docs/lib/op_systems/doc_opchanges/technote_glbstrato_20090618_en.pdf.
- Côté, J., Gravel, S., Méthot, A., Patoine, A., Roch, M., Staniforth, A., 1998a. The operational CMC–MRB global environmental multiscale (GEM) model, part I: design considerations and formulation. *Mon. Wea. Rev.* 126, 1373–1395. [dx.doi.org/10.1175/1520-0493\(1998\)126<1373:TOCMGE>2.0.CO;2](https://doi.org/10.1175/1520-0493(1998)126<1373:TOCMGE>2.0.CO;2).
- Côté, J., Desmarais, J.-G., Gravel, S., Méthot, A., Patoine, A., Roch, M., Staniforth, A., 1998b. The operational CMC–MRB global environmental multiscale (GEM) model. Part II: results. *Mon. Wea. Rev.* 126, 1397–1418. [dx.doi.org/10.1175/1520-0493\(1998\)126<1397:TOCMGE>2.0.CO;2](https://doi.org/10.1175/1520-0493(1998)126<1397:TOCMGE>2.0.CO;2).
- D'Amours, R., Malo, A., 2004. A Zeroth Order Lagrangian Particle Dispersion Model MLDPO. Internal Publication, Canadian Meteorological Centre, Environmental Emergency Response Section, Dorval, QC, Canada, 19 pp. <http://eer.cmc.ec.gc.ca/publications/DAmours.Malo.2004.CMC-EER.MLDPO.pdf>.
- D'Amours, R., Malo, A., Servranckx, R., Bensimon, D., Trudel, S., Gauthier, J.-P., 2010. Application of the atmospheric Lagrangian particle dispersion model MLDPO to the 2008 eruptions of Okmok and Kasatochi volcanoes. *J. Geophys. Res.* 115, D00L11. [dx.doi.org/10.1029/2009JD013602](https://doi.org/10.1029/2009JD013602).
- Davies, T., Cullen, M.J.P., Malcolm, A.J., Mawson, M.H., Staniforth, A., White, A.A., Wood, N., 2005. A new dynamical core for the Met Office's global and regional modelling of the atmosphere. *Q. J. R. Meteorol. Soc.* 131, 1759–1782. [dx.doi.org/10.1256/qj.04.101](https://doi.org/10.1256/qj.04.101).
- Draxler, R.R., 2006. The use of global and mesoscale meteorological model data to predict the transport and dispersion of tracer plumes over Washington, D.C. *Wea. Forecasting* 21, 383–394. [dx.doi.org/10.1175/WAF926.1](https://doi.org/10.1175/WAF926.1).
- Draxler, R.R., Hess, G.D., 1998. An overview of the HYSPLIT_4 modelling system for trajectories, dispersion, and deposition. *Aus. Meteorol. Mag.* 47, 295–308.
- Draxler, R.R., Hess, G.D., 1997. Description of the HYSPLIT_4 Modeling System. NOAA tech. memo. ERL ARL-224. Air Resources Laboratory, Silver Spring, MD, 24 pp., NTIS PB98-116593.
- Draxler, R.R., Rolph, G.D., 2012. Evaluation of the transfer coefficient matrix (TCM) approach to model the atmospheric radionuclide air concentrations from Fukushima. *J. Geophys. Res.* 117, D05107. [dx.doi.org/10.1029/2011JD017205](https://doi.org/10.1029/2011JD017205).
- Fox, D.G., 1984. Uncertainty in air quality modeling. *Bull. Am. Meteorol. Soc.* 65, 27–36. [dx.doi.org/10.1175/1520-0477\(1984\)065<0027:UAQM>2.0.CO;2](https://doi.org/10.1175/1520-0477(1984)065<0027:UAQM>2.0.CO;2).
- Furuta, S., Sumiya, S., Watanabe, H., et al., 2011. Results of the Environmental Radiation Monitoring Following the Accident at the Fukushima Daiichi Nuclear Power Plant – Interim Report (Ambient Radiation Dose Rate, Radioactivity Concentration in the Air and Radioactivity Concentration in the Fallout). Radiation Protection Department, Nuclear Fuel Cycle Engineering Laboratories, Tokai Research and Development Center, Japan Atomic Energy Agency, Tokaimura, Naka-gun, Ibaraki-ken. JAEA-review 2011-035. (in Japanese).
- Galmarini, S., Solazzo, E., 2014. The Fukushima-Cs137 deposition case study: properties of the multi-model ensemble. *J. Environ. Radioact.* 139, 226–233.
- Hanna, S.R., 1989. Confidence limits for air quality model evaluations, as estimated by bootstrap and jackknife resampling methods. *Atmos. Environ.* 23, 1385–1398. [dx.doi.org/10.1016/0004-6981\(89\)90161-3](https://doi.org/10.1016/0004-6981(89)90161-3).
- Hanna, S.R., 1993. Uncertainties in air quality model predictions. *Bound.-Layer Meteorol.* 62, 3–20. [dx.doi.org/10.1007/BF00705545](https://doi.org/10.1007/BF00705545).
- Hertel, O., Christensen, J., Runge, E.H., Asman, W.A.H., Berkowicz, R., Hovmand, M.F., Hov, O., 1995. Development and testing of a new variable scale air pollution model—ACDEP. *Atmos. Environ.* 29, 1267–1290. [dx.doi.org/10.1016/1352-2310\(95\)00067-9](https://doi.org/10.1016/1352-2310(95)00067-9).
- Honda, Y., Nishijima, M., Koizumi, K., Ohta, Y., Tamiya, K., Kawabata, T., Tsuyuki, T., 2005. A pre-operational variational data assimilation system for a non-hydrostatic model at the Japan Meteorological Agency: formulation and preliminary results. *Q. J. R. Meteorol. Soc.* 131, 3465–3475. [dx.doi.org/10.1256/qj.05.132](https://doi.org/10.1256/qj.05.132).
- Honda, Y., Sawada, K., 2008. A new 4D-Var for mesoscale analysis at the Japan Meteorological Agency. *CAS/JSC WGNE Res. Act. Atmos. Ocean. Model.* 38, 017–018.
- Jones, A.R., Thomson, D.J., Hort, M.C., Devenish, B., 2007. The U.K. Met Office's next-generation atmospheric dispersion model, NAME III. In: Borrego, C., Norman, A.L. (Eds.), *Air Pollution and Its Applications XVII, Proceedings of the 27th NATO/CCMS International Technical Meeting on Air Pollution Modelling and Its Application*. Springer, pp. 580–589.
- Kanamitsu, M., 1989. Description of the NMC global data assimilation and forecast system. *Wea. Forecasting* 4, 335–342. [dx.doi.org/10.1175/1520-0434\(1989\)004<0335:DOTNGD>2.0.CO;2](https://doi.org/10.1175/1520-0434(1989)004<0335:DOTNGD>2.0.CO;2).
- Kanamitsu, M., Alpert, J.C., Campana, K.A., Caplan, P.M., Deaven, D.G., Iredell, M., Katz, B., Pan, H.-L., Sela, J., White, G.H., 1991. Recent changes implemented into

- the global forecast system at NMC. *Wea. Forecasting* 6, 425–435. [dx.doi.org/10.1175/1520-0434\(1991\)006<0425:RCITGT>2.0.CO;2](https://doi.org/10.1175/1520-0434(1991)006<0425:RCITGT>2.0.CO;2).
- Katata, G., Terada, H., Nagai, H., Chino, M., 2012. Numerical reconstruction of high dose rate zones due to the Fukushima Dai-ichi nuclear power plant accident. *J. Environ. Radioact.* 111, 2–12.
- Kinoshita, N., Sueki, K., Sasa, K., Kitagawa, J.-I., Ikarashi, S., Nishimura, T., Wong, Y.-S., Satou, Y., Handa, K., Takahashi, T., Sato, M., Yamagata, T., 2011. Assessment of individual radionuclide distributions from the Fukushima nuclear accident covering central-east Japan. *Proc. Natl. Acad. Sci. U. S. A.* 108, 19526–19529. [http://dx.doi.org/10.1073/pnas.1111724108](https://doi.org/10.1073/pnas.1111724108).
- Kitada, T., 1994. *Modelling of Transport, Reaction and Deposition of Acid Rain*. Kishou Kenkyu note, 182, pp. 95–117 (in Japanese).
- Kobayashi, T., Nagai, H., Chino, M., Kawamura, H., 2013. Source term estimation of atmospheric release due to the Fukushima Dai-ichi nuclear power plant accident by atmospheric and oceanic dispersion simulations. *J. Nucl. Sci. Technol.* 50 (3), 255–264. [dx.doi.org/10.1080/00223131.2013.772449](https://doi.org/10.1080/00223131.2013.772449).
- Le Petit, G., Douyset, G., Ducros, G., Gross, P., Achim, P., Monfort, M., Raymond, P., Pontillon, Y., Jutier, C., Blanchard, X., Taffary, T., Moulin, C., 2012. Analysis of radionuclide releases from the Fukushima Dai-ichi nuclear power plant accident part I. *Pure Appl. Geophys.* [dx.doi.org/10.1007/s00024-012-0581-6](https://doi.org/10.1007/s00024-012-0581-6).
- Mahfouf, J.-F., Rabier, F., 2000. The ECMWF operational implementation of four-dimensional variational assimilation. II: experimental results with improved physics. *Q. J. R. Meteorol. Soc.* 126, 1171–1190. [dx.doi.org/10.1002/qj.49712656416](https://doi.org/10.1002/qj.49712656416).
- Maryon, R.H., Ryall, D.B., Malcolm, A.L., 1999. *The NAME 4 Dispersion Model: Science Documentation*. Technical report. UK Meteorological Office. Turbulence diffusion note no. 262.
- McMahon, T.A., Denison, P.J., 1979. Empirical atmospheric deposition parameters – a survey. *Atmos. Environ.* 13, 571–585.
- MEXT, 2011. http://www.mext.go.jp/b_menu/shingi/chousa/gijyutu/017/shiryo/_icsFiles/afieldfile/2011/09/02/1310688_1.pdf.
- Morino, Y., Ohara, T., Nishizawa, M., 2011. Atmospheric behavior, deposition, and budget of radioactive materials from the Fukushima Daiichi nuclear power plant in March 2011. *Geophys. Res. Lett.* 38, L00G11. [dx.doi.org/10.1029/2011GL048689](https://doi.org/10.1029/2011GL048689).
- Mosca, S., Graziani, G., Klug, W., Bellasio, R., Bianconi, R., 1998. A statistical methodology for the evaluation of long-range dispersion models: an application to the ETEX exercise. *Atmos. Environ.* 32, 4307–4324. [dx.doi.org/10.1016/S1352-2310\(98\)00179-4](https://doi.org/10.1016/S1352-2310(98)00179-4).
- Nagata, K., 2011. Quantitative Precipitation Estimation and Quantitative Precipitation Forecasting by the Japan Meteorological Agency. Technical review no. 13. RSMC Tokyo – Typhoon Center, pp. 37–50 <http://www.jma.go.jp/jma/jma-eng/jma-center/rsmc-hp-pub-eg/techrev/text13-2.pdf>.
- Ohkura, T., Oishi, T., Taki, M., et al., 2012. *Emergency Monitoring of Environmental Radiation and Atmospheric Radionuclides at Nuclear Science Research Institute, JAEA Following the Accident of Fukushima Daiichi Nuclear Power Plant*. Tokai Research and Development Center, Japan Atomic Energy Agency. JAEA-data/code 2012-010.
- Rabier, F., Järvinen, H., Klinker, E., Mahfouf, J.-F., Simmons, A., 2000. The ECMWF operational implementation of four-dimensional variational assimilation. I: experimental results with simplified physics. *Q. J. R. Meteorol. Soc.* 126, 1143–1170. [dx.doi.org/10.1002/qj.49712656415](https://doi.org/10.1002/qj.49712656415).
- Riccio, A., Ciaramella, A., Giunta, G., Galmarini, S., Solazzo, E., Potempski, S., 2012. On the systematic reduction of data complexity in multimodel atmospheric dispersion ensemble modeling. *J. Geophys. Res.* 117, D05314. [dx.doi.org/10.1029/2011JD016503](https://doi.org/10.1029/2011JD016503).
- Saito, K., 2012. The JMA nonhydrostatic model and its applications to operation and research (Chapter 5). In: Yucel, Ismail (Ed.), *Atmospheric Model Applications*, ISBN 978-953-51-0488-9, pp. 85–110 [dx.doi.org/10.5772/35368](https://doi.org/10.5772/35368).
- Saito, K., Ishida, J., Aranami, K., Hara, T., Segawa, T., Narita, M., Honda, Y., 2007. Nonhydrostatic atmospheric models and operational development at JMA. *J. Meteorol. Soc. Jpn.* 85B, 271–304. [dx.doi.org/10.2151/jmsj.85B.271](https://doi.org/10.2151/jmsj.85B.271).
- Saito, K., Shimbori, T., Draxler, R., 2014. JMA's regional ATM calculations for the WMO Technical Task Team on meteorological analyses for Fukushima Daiichi nuclear power plant accident. *J. Environ. Radioact.* 139, 185–199.
- Shimbori, T., Aikawa, Y., Fukui, K., Hashimoto, A., Seino, N., Yamasato, H., 2010. Quantitative tephra fall prediction with the JMA mesoscale tracer transport model for volcanic ash: a case study of the eruption at Asama volcano in 2009. *Pap. Meteorol. Geophys.* 61, 13–29. [dx.doi.org/10.2467/mripapers.61.13](https://doi.org/10.2467/mripapers.61.13).
- Simmons, A.J., Burridge, D.M., Jarraud, M., Girard, C., Wergen, W., 1989. The ECMWF medium-range prediction models: development of the numerical formulations and the impact of increased resolution. *Meteorol. Atmos. Phys.* 40, 28–60. [dx.doi.org/10.1007/BF01027467](https://doi.org/10.1007/BF01027467).
- Stohl, A., Forster, C., Frank, A., Seibert, P., Wotawa, G., 2005. Technical note: the Lagrangian particle dispersion model FLEXPART version 6.2. *Atmos. Chem. Phys.* 5, 2461–2474. [dx.doi.org/10.5194/acp-5-2461-2005](https://doi.org/10.5194/acp-5-2461-2005).
- Stohl, A., Seibert, P., Wotawa, G., Arnold, D., Burkhart, J.F., Eckhardt, S., Tapia, C., Vargas, A., Yasunari, T.J., 2012. Xenon-133 and caesium-137 releases into the atmosphere from the Fukushima Daiichi nuclear power plant: determination of the source term, atmospheric dispersion, and deposition. *Atmos. Chem. Phys.* 12, 2313–2343. [dx.doi.org/10.5194/acp-12-2313-2012](https://doi.org/10.5194/acp-12-2313-2012).
- Stohl, A., Hittenberger, M., Wotawa, G., 1998. Validation of the Lagrangian particle dispersion model FLEXPART against large-scale tracer experiment data. *Atmos. Environ.* 32, 4245–4264. [dx.doi.org/10.1016/S1352-2310\(98\)00184-8](https://doi.org/10.1016/S1352-2310(98)00184-8).
- Sugiyama, G., Nasstrom, J., Pobanz, B., Foster, K., Simpson, M., Vogt, P., Aluzzi, F., Homann, S., 2012. Atmospheric dispersion modeling: challenges of the Fukushima Daiichi response. *Health Phys.* 102, 493–508. [dx.doi.org/10.1097/HP.0b013e31824c7bc9](https://doi.org/10.1097/HP.0b013e31824c7bc9).
- Takemura, T., Nakamura, H., Takigawa, M., Kondo, H., Satomura, T., Miyasaka, T., Nakajima, T., 2011. A numerical simulation of global transport of atmospheric particles emitted from the Fukushima Daiichi nuclear power plant. *Sci. Online Lett. Atmos.* 7, 101–104. [dx.doi.org/10.2151/sola.2011-026](https://doi.org/10.2151/sola.2011-026).
- Terada, H., Katata, G., Chino, M., Nagai, H., 2012. Atmospheric discharge and dispersion of radionuclides during the Fukushima Dai-ichi nuclear power plant accident. Part II: verification of the source term and analysis of regional-scale atmospheric dispersion. *J. Environ. Radioact.* 112, 141–154. [dx.doi.org/10.1016/j.jenvrad.2012.05.023](https://doi.org/10.1016/j.jenvrad.2012.05.023).
- USDOE, 2011. United States Department of Energy. <https://explore.data.gov/d/prmn-6s35>.
- WMO, 2013. The World Meteorological Organization's Evaluation of Meteorological Analyses for the Radionuclide Dispersion and Deposition from the Fukushima Daiichi Nuclear Power Plant Accident. Report on the third meeting of the WMO Task Team on meteorological analyses for the Fukushima-Daiichi nuclear power plant accident, annex III http://www.wmo.int/pages/prog/www/CBS-Reports/documents/WMO_fnpp_final_AnnexIII_4Feb2013_REVISIED_17June2013.pdf.
- Yasunari, T.J., Stohl, A., Hayano, R.S., Burkhart, J.F., Eckhardt, S., Yasunari, T., 2011. Cesium-137 deposition and contamination of Japanese soils due to the Fukushima nuclear accident. *Proc. Natl. Acad. Sci. U. S. A.* 108 (49), 19530–19534. [dx.doi.org/10.1073/pnas.1112058108](https://doi.org/10.1073/pnas.1112058108).